Transactions on Computational and Scientific Methods | Vol4, No. 8, 2024
ISSN: 2998-8780
https://pspress.org/index.php/tcsm
Pinnacle Science Press

Machine Vision-Based Tenon Size Detection for Aero-Engine Blades Using Enhanced Edge Detection and Fitting Algorithms

Merrick Hale
Department of Mechanical Engineering, University of Delaware, USA
merrick.hale83@udel.edu

Abstract: Accurate dimension detection of the tenon in aero-engine blades is critical to ensuring proper fitting and performance. Traditional methods, such as the enlarged projection technique, are becoming inadequate as the demand for qualified blades grows. This paper presents a machine vision detection system designed to address the limitations of current tenon size detection methods. The system employs an improved bilateral filtering adaptive Canny operator for edge detection and combines Hough transform with least squares for edge fitting. The proposed algorithm enhances the accuracy of tenon dimension detection by retaining more edge feature information and adjusting the threshold adaptively to match image features. Experimental results show that the method achieves higher precision and execution efficiency compared to traditional techniques, providing more reliable contour detection results. Despite its success, further improvements in image acquisition quality and edge extraction accuracy will be pursued to meet the increasing demand for precision in future applications.

Keywords: Aero-engine Blade; Tenon; Edge Fitting.

1. Introduction

The blade is an essential part of the aero-engine, composed of the blade body and tenon [1,2]. The blade is fixed on the engine through the fitting of tenon and mortise. If the tenon size is unqualified, there may be a risk of failure to fit or falling off. The current traditional tenon size detection method is the enlarged projection method. The judgment is made by visually observing and comparing the measured tenon profile and the standard tenon profile under the enlarged projection. As the demand for qualified blades continues to expand, the traditional detection method is no longer applicable, and the rapid detection of the tenon size has become an urgent problem to be solved.

Machine vision technology [3], which simulates human visual function through digital image processing, has been widely used in size detection [4]. With its non-contact and digital characteristics, it can significantly improve the execution efficiency of reviews. Ngoc Vu Ngo et al. used a three-dimensional measurement system to obtain its feature points in the world coordinate system to calculate the measurement data [5]. Junhui Huang et al. hole radius and spacing measurement method is presented based on binocular vision combined with dynamic local plane for the large-size workpiece with plane feature [6]. Jia L put forward an Image feature recognition method based on the Hough transform, and the size detection algorithm is designed on this basis [7].

Through previous studies, it can be found that using the Canny[8,9] operator and curve fitting helps detect various edge cases; Profile detection can be done by edge detection, which has the potential to realize the dimension detection of blade tenons. However, there is still much room for improvement in the detection accuracy of the current method. Therefore, in this paper, a machine vision detection

system for blade tenon size is designed. The detection platform collects the image of the tenon and obtains the detection results according to the corresponding detection algorithm designed. The detection algorithm is particularly critical. First, accurate edge features are obtained based on improved bilateral filtering adaptive Canny operator, and then edge curves are fitted by combining Hough detection and least squares. Finally, the calculation and detection of tenon size are completed.

2. Detection System Design

The detection system mainly includes two parts: hardware system and software algorithm. The hardware system is used to obtain clear and reliable blade tenon images and save the images to the computing storage unit; the software is used primarily to complete image analysis and output detection results.

2.1. Hardware Structure

The blade tenon of an aero-engine is shown in Fig. 1(a), which adopts the most widely used fir tree structure in turbines. The two ends are in the shape of a giant wedge and a small wedge. The wedge shape occupies a smaller circumferential dimension on the wheel rim, so more blades can be installed. The blades are also easy to disassemble and replace. There are symmetrically distributed semicircular mortise teeth on both sides of the mortise, which can fit with the inverted wedge-shaped mortise and groove of the same profile on the wheel rim.



(a) blade tenon (b) Image acquisition device

Figure 1. Detection system hardware

The image acquisition device of the blade tenon is shown in Figure 1(b), which consists of a camera, a lens, a light source, and a computer. The camera adopts the Newhall company model DZ-9288 industrial camera; the camera resolution is 4000*3000. In addition to the camera, a suitable light source type and lighting method are conducive to acquiring high-quality images. Compared with top-light ring lighting, parallel backlight lighting can produce images with sharp edges and fewer transition pixels at the border. Therefore, the lighting method adopts Parallel backlighting for sharp-edge images.

2.2. System Software Structure

The processing after image acquisition needs to be completed by the software system. This research uses Python language and Opencv library Design and implements related algorithms, and the detection algorithm flow of the blade tenon is shown in Figure 2.

Algorithm flow: First, grayscale the collected image of the tenon; use the adaptive edge operator of bilateral filtering to extract the edge pixels of the tenon; use the Hough transform to detect the straight line in the edge initially, and segment and filter the edge points; Then use the least square method to fit precise straight lines and circles; finally calculate the dimensions of each part of the tenon according to the geometric relationship.

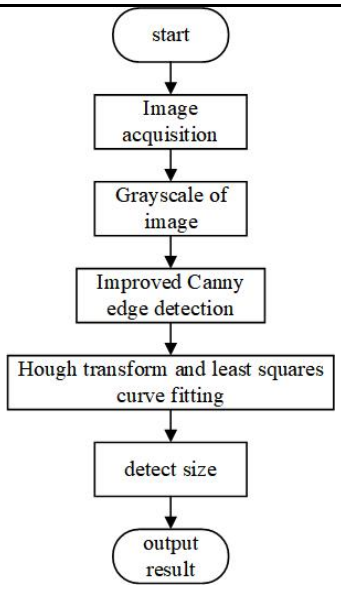


Figure 2. Detection algorithm flow

3. The Key Algorithm of Blade Tenon Detection

3.1. Improved Edge Detection

Bilateral filtering is developed based on Gaussian filtering[10]. When sampling, the spatial distance of pixels is considered, and the grey similarity of pixels is added. Compared with Gaussian filtering, this combination of spatial proximity and The weighted processing of the parallel with the grey value can make the filter kernel change non-linearly according to different grey values at different positions in the image. This weighted method, which considers spatial information and grey similarity simultaneously, achieves the purpose of edge preservation and denoising and has the characteristics of simple, non-iterative, and local processing. Therefore, the effect of maintaining edges and smoothing noise reduction can be achieved. The bilateral filtering formula is as follows:

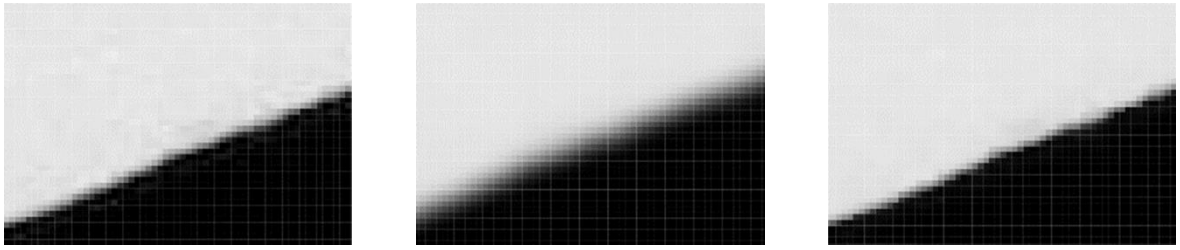
$$\bar{I}(p) = \frac{1}{W_p}\sum_{q\in S} G_{\sigma_s}(\|p-q\|)G_{\sigma_r}(|I(p)-I(q)|)I(q)$$

$$W_p = \sum_{q\in S} G_{\sigma_s}(\|p-q\|)G_{\sigma_r}(|I(p)-I(q)|)$$

$$G_{\sigma_s}(\|p-q\|) = e^{-\frac{(i-m)^2+(j-n)^2}{2\sigma_S^2}}$$

$$G_{\sigma_r}(|I(p)-I(q)|) = e^{-\frac{[I(i,j)-I(m,n)]^2}{2\sigma_r^2}}$$

q represents the adjacent pixel, The (m, n) represents the coordinates of the adjacent pixel, I(m, n) represents the value of the adjacent pixel, p represents the central pixel, (i, j) the coordinates of the central pixel, I(i, j) represents the value of the centre pixel. G_{σ_s} calculates the space domain, G_{σ_r} calculates the pixel domain and traverses each image pixel to obtain the filtering result.



(a) Original picture details (b) Gaussian filter (d) Bilateral filter

Figure 3. Filtering effect of blade tenon image

The filtering effects of Sissian and bilateral filtering are shown in Figure 3. Although the noise is eliminated after Gaussian filtering, the edge part of the image is blurred to a certain extent, which has a particular impact on the edge extraction. The bilateral filtering algorithm preserves the edge contour well while removing the image noise, so this paper replaces the Gaussian filtering in the traditional Canny algorithm with bilateral filtering.

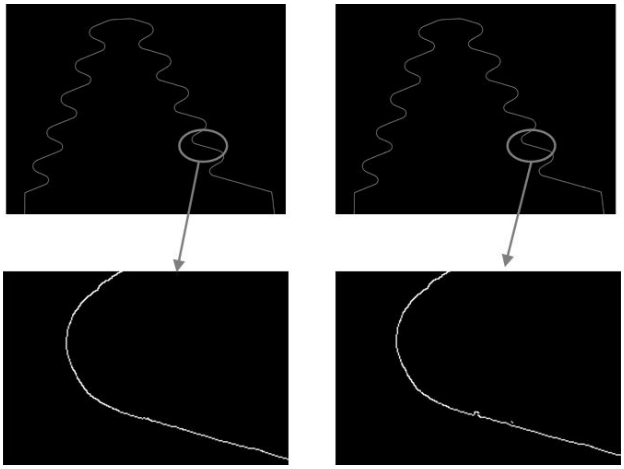
The maximum between-class variance method is based on the grey histogram information of the image to complete the threshold selection automatically. Assuming a target image with a size of M × M, the grey value range is [0, L — 1], and the pixels whose grey value is less than t in the imageare classified into a class C0, that is, [0, t] ∈ C0, and the rest The pixels are organized into a class C1, that is, [t + 1, L — 1] ∈ C1, the formula is as follows:

$$P_0(t) = \sum_{i=1}^{t} P_i$$
$$P_1(t) = \sum_{i=t+1}^{L-1} P_i = 1 - P_0(t)$$
$$u_0(t) = \sum_{i=0}^{t} \left(i \frac{P_i}{P_0(t)} \right)$$
$$u_1(t) = \sum_{i=t+1}^{L-1} \left(i \frac{P_i}{P_0(t)} \right)$$

In the formula, i represents the grey value, P_i is the probability of occurrence of grey value i, $P_0(t)$, $P_1(t)$ represent the probability of occurrence of categories C0 and C1, respectively, $u_0(t)$, $u_1(t)$ represent the probability of category C0 , the average grey level of C1. According to the above results, the inter-class variance expression of the image can be obtained as follows:

$$\sigma(t) = P_0(t)u_0^2(t) + P_1(t)u_1^2(t)$$

The segmentation threshold when the inter-class variance is the largest is taken as the high threshold T_h, and the low threshold is T_l=T_h/2



(a) Improved Canny (b) Canny

Figure 4. Canny improved before and after the effect comparison

The maximum inter-class variance method obtains the adaptive threshold, which can avoid the traditional manual setting and adapt well to different light environments, enhancing the algorithm's robustness and providing a good foundation for subsequent size detection.

Table 1: Edge detection performance index comparison

Algorithm	P	R	F1
Canny	0.8905	0.9062	0.8983
Improved Canny	0.9137	0.9229	0.9183

4. Experimental Results

According to the detection requirements, it is necessary to inspect the cross-rod distance, tenon width, tooth shape and wedge angle of the tenon and compare the average result of five detections with the processing design value of the tenon.

(1) Cross-rod distance detection. The rod span is an indirect parameter representing the tooth thickness. Use two measuring rods to clamp in the opposite tooth grooves to measure the size of the outer edge. Generate a virtual measuring rod with a known radius according to the requirements of the detection process, make the measuring rod tangent to the two sides of the tooth groove, and then calculate the distance between the centres of the two virtual measuring rods plus the diameter to obtain the distance between the rods:

$$d_{Æ} = \sqrt{(x_1 — x_2)^2 + (y_1 — y_2)^2} + 2r_l$$

Among them, (x_1, y_1) , (x_2, y_2) are the centre positions of the two virtual measuring sticks respectively, and r_l is the radius of the measuring stick. For each level of tongue and groove detection, the detection results are shown in Table 2.

Table 2: Cross-rod distance detection

Tooth level	True value	Number of detections					Average test results	Error value
		1	2	3	4	5		
1	11.095	11.0738	11.0752	11.0732	11.0746	11.0804	11.07544	-0.01956
2	9.359	9.3434	9.3574	9.3422	9.3485	9.3537	9.34904	-0.00996
3	7.623	7.6098	7.6005	7.6155	7.6024	7.6128	7.6082	-0.0148
4	5.887	5.8796	5.8817	5.8915	5.8818	5.8828	5.88348	-0.00352
5	4.151	4.1437	4.1529	4.1468	4.1425	4.1532	4.14782	-0.00318

Table 3: Tenon width detection

tenon width level	True value	Number of detections					Average test results	Error value
		1	2	3	4	5		
1	9.836	9.8185	9.8153	9.8214	9.8175	9.8196	9.81846	-0.01754
2	8.1	8.0874	8.0912	8.0897	8.0863	8.0887	8.08866	-0.01134
3	6.364	6.3574	6.3594	6.3621	6.3558	6.3592	6.35878	-0.00522
4	4.628	4.6263	4.6351	4.6318	4.6174	4.6155	4.62522	-0.00278
5	2.892	2.8923	2.9152	2.8875	2.8764	2.8971	2.8937	0.0017

Table 4: Detection of the addendum circle radius

Number of circles	True value	Number of detections					Average test results	Error value
		1	2	3	4	5		
1	0.35	0.3288	0.3265	0.3281	0.3275	0.3327	0.32872	-0.02128
2		0.3271	0.3261	0.3284	0.3312	0.3261	0.32778	-0.02222
3		0.3211	0.3235	0.3247	0.3238	0.3284	0.3243	-0.0257
4		0.3269	0.3278	0.324	0.3264	0.3226	0.32554	-0.02446
5		0.3142	0.3258	0.3262	0.3286	0.3189	0.32674	-0.02326
6		0.3220	0.3216	0.3293	0.3274	0.3263	0.32532	-0.02468

7		0.3264	0.3221	0.3237	0.3216	0.3275	0.32426	-0.02574
8		0.3254	0.3284	0.3244	0.3257	0.3243	0.32564	-0.02436
9		0.3211	0.3295	0.3206	0.3248	0.3284	0.32488	-0.02512
10		0.3177	0.3239	0.3221	0.3252	0.3266	0.3231	-0.0269

(2) The intersection point of the pitch line and the working surface of the tenon is the node, and the distance between the two nodes on the same level tenon is the tenon width. The detection results of the tenon width of each level are in Table 3.

(3) Tooth shape detection: Tooth shape includes the detection of the tooth pitch, addendum circle and dedendum circle of each tenon tooth. The position and radius of the addendum circle and the tooth bottom circle can be directly obtained during the fitting process. The detection results of the addendum circle and the dedendum circle radius are shown in Table 4 and Table 5, respectively. The tooth pitch is calculated by the distance between two adjacent tooth nodes. The detection results are in Table 6.

(4) Wedge angle detection. The wedge angle is the angle between the two pitch lines of the tenon. The wedge angle's size will affect the tenon's bearing capacity. The test results are in Table 7.

Table 5: Detection of the dedendum circle radius

Number of circles	True value	Number of detections					Average test results	Error value
		1	2	3	4	5		
1	0.24	0.2493	0.2453	0.2445	0.2532	0.2431	0.24708	0.00708
2		0.2441	0.2428	0.2462	0.2455	0.2487	0.24546	0.00546
3		0.2494	0.2459	0.2481	0.2476	0.2425	0.2467	0.0067
4		0.2528	0.2498	0.2483	0.2549	0.2514	0.25144	0.01144
5		0.2521	0.2477	0.2472	0.2536	0.2497	0.25006	0.01006
6		0.2373	0.2457	0.2416	0.2382	0.2439	0.24134	0.00134
7		0.2405	0.2462	0.2419	0.2397	0.2428	0.24222	0.00222
8		0.2455	0.247	0.2437	0.2481	0.2406	0.24498	0.00498
9		0.2448	0.2428	0.2442	0.2415	0.2456	0.24378	0.00378
10		0.2385	0.2436	0.2458	0.2396	0.2441	0.24232	0.00232

Table 6: Detection of the tooth pitch

Number of tooth pitch	True value	Number of detections					Average test results	Error value
		1	2	3	4	5		
1	1.98	1.9713	1.9724	1.9716	1.9748	1.9731	1.97264	-0.00736
2		1.9747	1.9738	1.9754	1.9742	1.9722	1.97406	-0.00594
3		1.9773	1.9792	1.9764	1.9758	1.9782	1.97738	-0.00262
4		1.9816	1.9793	1.978	1.9825	1.9767	1.97962	-0.00038
5		1.9764	1.9751	1.9776	1.9759	1.9786	1.97672	-0.00328
6		1.9779	1.9782	1.9827	1.9746	1.9756	1.9778	-0.0022
7		1.9797	1.9763	1.9784	1.9759	1.9808	1.97822	-0.00178
8		1.9793	1.9755	1.9746	1.9771	1.9753	1.97636	-0.00364

In the size detection, the length error of each part of the tenon is less than 0.03mm, and the wedge angle error is 0.056 degrees, which meets the current actual detection needs. In addition, compared with traditional manual detection, the visual detection method is more suitable for large-scale, non-contact detection and meets the actual needs of automatic industrial detection.

Table 7: Detection of the wedge angle

Number of wedge angle	True value	Number of detections					Average test results	Error value
		1	2	3	4	5		
8	52	51.95	51.92	51.95	51.96	51.94	51.944	-0.056

5. Conclusion

In order to solve the problem of dimension detection of the tenon of the aero-engine blade, in this paper, a machine vision detection system for the tenon size of aero-engine blades is designed. After the system collects the blade tenon image, the algorithm proposed in this paper is used to measure the overall dimension. In this method, the Gaussian filtering method of the Canny operator is changed to the bilateral filtering method, which retains more edge feature information in the image; at the same time, the maximum inter-class variance method is used to form an adaptive Canny operator threshold, which avoids The artificial setting of the relevant threshold makes the threshold more match the edge features of the image; secondly, the edge fitting method is established by combining Hough transform, and least squares, which solves the problem of low fitting accuracy of Hough transform and least squares Multiplication cannot segment the straight line primitives of the edge, which improves the effect of edge fitting. Compared with traditional methods, our proposed method has higher dimension detection accuracy, more reliable contour dimension detection results, and higher detection execution efficiency.

However, with the gradual increase in the demand for precise detection and accurate detection of aero-engine blade tenons, there is still room for improvement and improvement in the image acquisition quality, edge extraction accuracy, and size detection accuracy of our method. These issues will be addressed in our follow-up work to improve further.

References

[1] Sun B, Li B. A rapid method to achieve aero-engine blade form detection[J]. Sensors, 2015, 15(6): 12782-12801.

[2] Li D, Li Y, Xie Q, et al. Tiny defect detection in high-resolution aero-engine blade images via a coarse-to-fine framework[J]. IEEE Transactions on Instrumentation and Measurement, 2021, 70: 1-12.

[3] Golnabi H, Asadpour A. Design and application of industrial machine vision systems[J]. Robotics and Computer-Integrated Manufacturing, 2007, 23(6): 630-637.

[4] Zhao Yuanyuan. Application of Computer-based Machine Vision Measurement System in Industrial On-line Detection[J]. Journal of Physics: Conference Series,2021,1992(2).

[5] Ngo N V, Hsu Q C, Hsiao W L, et al. Development of a simple three-dimensional machine-vision measurement system for in-process mechanical parts[J]. Advances in Mechanical Engineering, 2017, 9(10): 1687814017717183.

[6] Huang J, Qi M, Wang Z, et al. High precision measurement for the chamfered hole radius and spacing of a large-size workpiece based on binocular vision combined with plane dynamic adjustment[J]. Applied Optics, 2021, 60(29): 9232-9240.

[7] Jia L. Research on Key Dimension Detection Algorithm of Auto Parts Based on Hough Transformation [C]//Proceedings of the 2019 International Conference on Robotics, Intelligent Control and Artificial Intelligence. 2019: 184-188.

[8] Canny J. A computational approach to edge detection[J]. IEEE Transactions on pattern analysis and machine intelligence, 1986 (6): 679-698.

[9] Meng Y, Zhang Z, Yin H, et al. Automatic detection of particle size distribution by image analysis based

on local adaptive canny edge detection and modified circular Hough transform[J]. Micron, 2018, 106: 34-41.

[10] Gavaskar R G, Chaudhury K N. Fast adaptive bilateral filtering[J]. IEEE Transactions on Image Processing, 2018, 28(2): 779-790.

[11] Gavin H P. The Levenberg-Marquardt algorithm for nonlinear least squares curve-fitting problems[J]. Department of Civil and Environmental Engineering, Duke University, 2019, 19.

[12] Barbosa W O, Vieira A W. On the improvement of multiple circles detection from images using hough transform[J]. TEMA (São Carlos), 2019, 20: 331-342.